

Climate and vegetation reconstructions using ice cores in lava tubes at El Malpais National Monument

Final Report

September 1, 2019

The Southwest United States has had a history of droughts and climatic hardship long before the occurrence of large scale anthropogenic related climate changes (Grissino-Mayer, 1995; Carrillo et al., 2017). Better understanding the climate of the past few thousand years in this region not only sheds light on the struggles faced by the Native Americans and early settlers of the Southwest, but may also give us insight into the problems affecting our society in the present and near future. Paleoclimate reconstructions are generated using proxies preserved in biological or inorganic archives that maintain evidence of past climate conditions. New archives are continually sought out by researchers to obtain a more complete picture of our planet's climatic past (Lowe & Walker, 2015).

For this research project we have obtained ice samples from three different lava tubes in the El Malpais National Monument (hereafter ELMA). The goals of this project was to answer the following research questions:

- 1) How do moisture source and temperature anomalies combine to produce the droughts and pluvials in the SW US?
- 2) What are the relative contributions of winter versus summer monsoon variations to SW megadrought and pluvial periods?
- 3) How can our refined understanding of drought and its drivers improve estimates of future drought risk?

In order to address all of the above, a team composed of PI (Onac), a Masters student (Parmenter) from the University of South Florida (USF), and three specialists from ELMA (S.

Baumann, E. Weaver, L. Sturtz) visited three lava tubes in the ELMA and collected the following samples: two 1-m long ice cores using a Kovacs Mark 3 (COS-710-002) ice corer from caves 29 and 95, respectively, and 60 sample from a 120 cm ice wall in Cave 455.



Fig. 1. Coring the ice deposit in Cave 29.

The ice cores were photographed, described, and sub-sampled while in the

cave to prevent melting. Each core was divided in slabs at 5-cm resolution and every individual ice sample was placed in a zipped bag, and allowed to melt at room temperature. After ice melted, the water was transferred into high-density polyethylene bottles and shipped to the USF Stable Isotope Lab in Tampa, FL.

Large charcoal samples from the upper part of the cores, specifically at 1.5, 20, 30, 48, and 55 cm depths (Fig. 2 left), were recovered from the ice-melted water and sent to the National Institute for Physics and Nuclear Engineering in Romania, for radiocarbon dating measurements using a 1 MV Tandetron accelerator mass spectrometer. This step was essential in obtaining a reliable absolute chronology, so that the isotope time series can be framed in a temporal context.



*Fig. 2. Ice cores from Cave 29; **Left**: test core; **Right**: full 1-m long ice core.*

The ice deposit in the third lava tube could not be cored due to low ceiling of the passage, but instead, ice samples were recovered at 2-cm interval from a 120 cm vertical ice wall using Petzl ice screws (Fig. 3). Since the ice was free of any organics, no samples for radiocarbon dating were available from this lava tube.

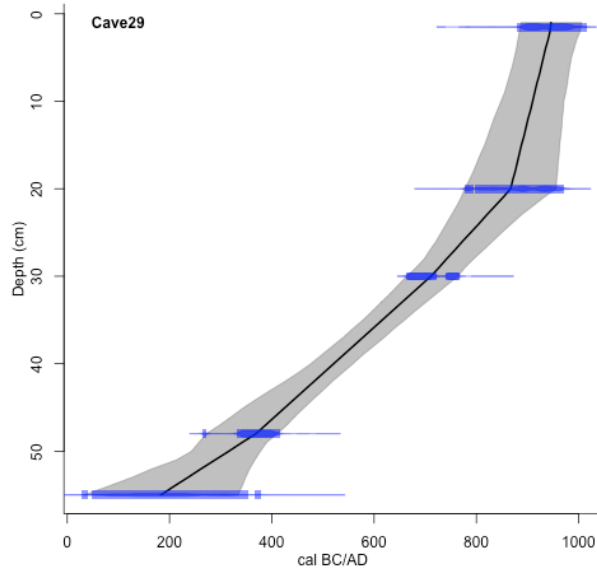


*Fig. 3. **Left**: The ice wall in Cave 455. **Right**: Recovering short, horizontal ice cores at 2-cm intervals.*

Age-depth modeling

The radiocarbon dating method depends on atmospheric ^{14}C concentrations, which varies throughout time. Because nuclear testing in the 1950s dramatically altered these concentrations, calibration techniques using U-series dated carbonates and tree rings with known ages must be employed. Age-depth models were created using the Clam 2.2 code (Blaauw, 2010) run under R (version 3.01), an open-source statistical software (R Development Core Team, 2013).

In this report we include the age-depth model for Cave 29 (Fig. 4), from which we inferred



that the ice at 55 cm in depth begun to accumulate around AD 100 (some 1,919 years ago) and continued until ~AD 1000. Since photographs taken in this lava tube in the early 80s show a much thicker ice deposit, we believe that part of the most recent ice (last 1,000 years) might have been lost due to global warming. Furthermore, the base of the ice must be much older but in the absence of charcoal, dating of the lower section was impossible at this time.

Fig. 4. The age-depth model for the ice deposit in Cave 29.

Oxygen ($\delta^{18}O$) and hydrogen (δ^2H) stable isotope record

The first step was to filter about 0.8 mL of ice-melted water using 0.22 μm Polytetrafluoroethylene disk filters before filling the 2 mL glass vials. The isotopic analyses were performed using a Piccaro L2130-i Cavity Ringdown Spectroscope at the Stable Isotope Lab (USF).

The $\delta^{18}O$ values for all three ice cores range between -5.7 and -12.2‰ and average -8.6‰. Cave 91 shows a decreasing trend for the first 25 cm (with the exception of the section between 15 and 20 cm) and relatively stable values, averaging -9.3‰, throughout the rest of the core (Fig. 5A). The ice core from Cave 29 (Fig. 5B) displays similar decreasing values for the first 27 cm from (-6.92 to -9.32‰). An overall increasing trend continues until 65 cm, when values plummet to the second lowest trough at -8.2‰. $\delta^{18}O$ values then increase for the remainder of the core with the highest peak of -5.7‰ at a depth of 90-95 cm. The most notable feature of the $\delta^{18}O$ results for Cave 455 (Supplementary Table 3) is the large shift to more negative values between 34-48 cm depth (Fig. 5C). $\delta^{18}O$ values throughout the core oscillate between -11.38 and -7.60‰, except for the depth interval mentioned above when they decrease as low as -12.45‰.

Based on these results, we produced plots (see Fig. 5 below) to identify fluctuations in the isotopic composition of oxygen. These are telling us the source of the rainfalls (Pacific vs Gulf of Mexico) in the area over the time period the ice accumulated. Combined with the radiocarbon ages we will be able to reconstruct the climate changes for ~900 years (between AD 100 and AD 1000) in the ELMA and SW USA.

The ice $\delta^{18}O$ time series for Cave 29 reveals an overall decreasing trend until the second largest trough (-8.9‰) at AD 502 (Fig. 6). This is followed by a brief increase before plummeting to the lowest point at -9.3‰ (~AD 666). The remainder of the core displays an overall increasing trend with its highest peak of -6.9‰ at AD 919.

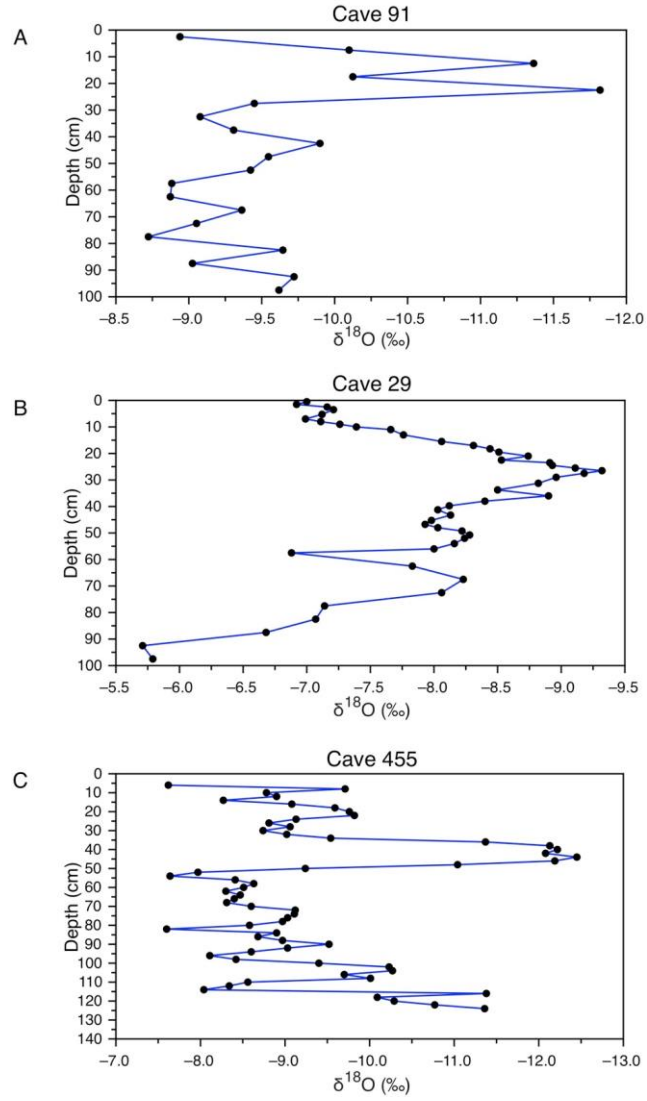


Fig. 5. $\delta^{18}\text{O}$ vs Depth models for cave 91 (A), 29 (B), and 455 (C) ice cores.

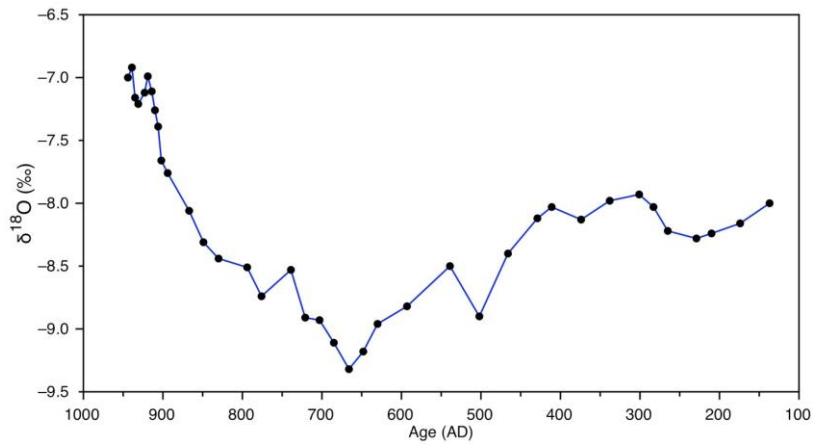


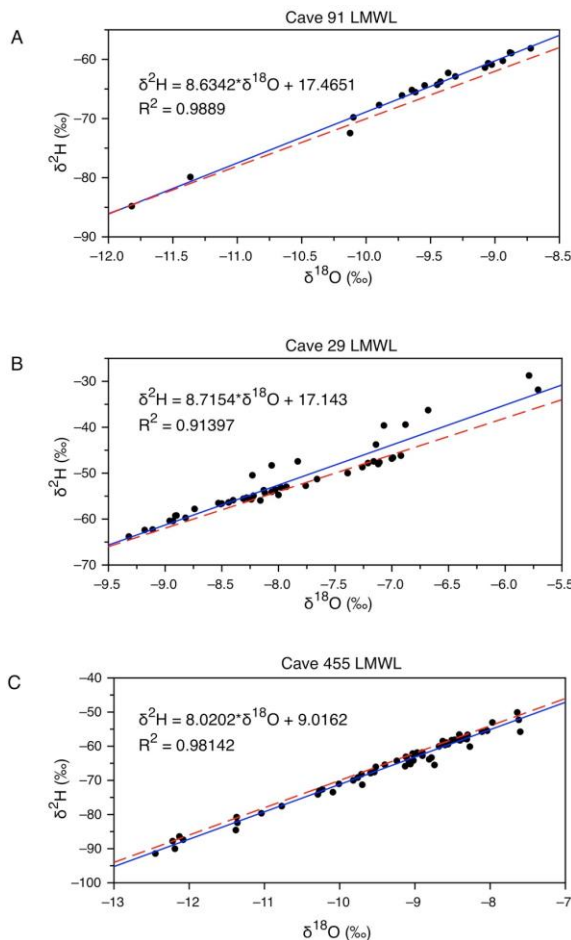
Fig. 6. The $\delta^{18}\text{O}$ time series plot for Cave 29.

The average oxygen and hydrogen stable isotope ratios in meteoric waters are expected to have a linear relationship, described by the so-called Meteoric Water Line. A Local Meteoric Water Line (LMWL) can be established for a specific location and its equation is then compared to the one of the Global Meteoric Water Line (GMWL) of non-evaporated meteoric water (Gat, 2010).

$$\delta^2\text{H} = 8 \cdot \delta^{18}\text{O} + 10 \text{ (‰)}$$

The $\delta^2\text{H}$ values across all cores have a minimum of -91.4‰ and a maximum of -28.7‰, with a mean of -59.1‰. LMWLs plotted for all three cores show good linear correlations with R^2 values > 0.90 . The Cave 91 LMWL (Fig. 7A) displays a positive linear correlation between $\delta^2\text{H}$ and $\delta^{18}\text{O}$ values with an R^2 of 0.9889. The equation given by this relationship plots above the GMWL with a much higher d-excess of 17.5‰. The LMWL plot obtained from Cave 29 (Fig. 7B) has an R^2 of 0.91317 and plots above the GMWL, but with a higher slope of 8.7. The d-excess obtained from this core approximates that of Cave 29 at 17.14. Cave 455 has a LMWL (Fig. 7C) that bears the closest resemblance to the GMWL with a slope of 8.02 and a d-excess of 9.01, with a good linear relationship defined by $R^2=0.98142$.

The LMWL from Cave 455 has a slope that nearly matches that of the GMWL. Variations in LMWL slope indicate evaporative processes during precipitation (Rozanski et al., 1993). Therefore, we can assume that the ice in Cave 455 was subject to little or no evaporation during precipitation. The d-excess value of 9.01 is slightly lower than the GMWL. This suggest slightly



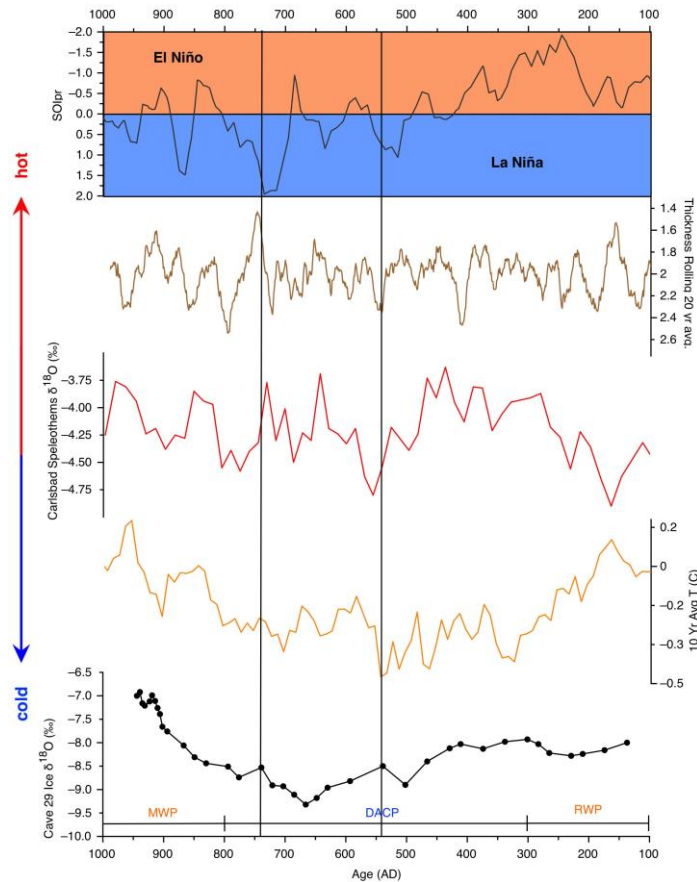
higher relative humidity at the moisture source compared to that of nearby land. The LMWL derived from the Cave 91 ice core is defined by the equation $\delta^2\text{H} = 8.6 \cdot \delta^{18}\text{O} + 17.5$. The slightly higher slope here (relative to the GMWL) signifies a small amount of evaporation during precipitation. A large d-excess of 17.5 infers a substantially lower relative humidity at moisture source. This could indicate a different primary moisture source from the ice in Cave 455, or it could be the result of ice accumulation during an extended period of arid conditions at the same source.

Fig. 7. The Local Meteoric Water Line for Cave 91 (A), 29 (B), and 455 (C) ice cores (blue line) plotted against the GMWL (red dashed line).

The Cave 29 $\delta^{18}\text{O}$ record and major climate events

The upper 55 cm of the Cave 29 ice core spans the period between ~AD 100 and 1000. There are three important climate events that cover this interval: the Roman Warm Period (RWP: AD 50-300), Dark Ages Cold Period (DACP: AD 300-800), and the Medieval Warm Period (MWP: AD 800-1300). $\delta^{18}\text{O}$ values in our core remain relatively constant throughout the RWP, and immediately plunge prior the onset of the DACP at AD ~450. A steady increasing trend begins around AD 665, accelerating at the beginning of the MWP (AD ~850). We found several other proxy records that span these climate periods for use in comparison (Fig. 8).

In understanding the relationship between our $\delta^{18}\text{O}$ values and temperature trends, we use the Ljungqvist (2010) multi-proxy reconstruction of Northern Hemisphere temperature (blue line). While major peaks and troughs have little in common between records, our values do follow general Northern Hemisphere temperature trends, allowing to distinguish three distinct climate periods (RWP, DACP, and MWP). Our record, however, appears to have a delayed response to these large



scale temperature changes.

Fig. 8. A comparison between the Cave 29 ice core $\delta^{18}\text{O}$ record (black line), the Northern hemisphere multi-proxy temperature reconstruction (blue line) (Ljungqvist, 2010), the Grissino-Mayer (1995) El Malpais tree-ring thickness record (brown line), Carlsbad speleothem $\delta^{18}\text{O}$ record (red line) (Asmerom et al., 2007), and

the Southern Oscillation Index reconstruction by Yan et al. (2011) (orange line). Major climate regimes are identified above the bottom x-axis (see text for abbreviations used).

One way of discerning how much the amount effect controls variations in $\delta^{18}\text{O}$ values in El Malpais precipitation records is to inspect the dendrochronology study provided by Grissino-Mayer (1995) (Fig. 8 brown line). As precipitation amount has an inverse relationship with $\delta^{18}\text{O}$, the tree-ring growth scale used in our figure for the El Malpais record has been reversed. A close inspection of the trends in this record as compared to the Carlsbad Caverns speleothem $\delta^{18}\text{O}$ record by Asmerom et al. (2007) (Fig. 8 red line) reveals an inverse relationship for many of the peaks, confirming a certain amount of variability in $\delta^{18}\text{O}$ values in speleothems due to the amount effect. In these records, increases in precipitation denoted by tree ring growth often correspond with decreases in $\delta^{18}\text{O}$. One reason why this relationship is not consistent throughout the record could possibly be due to the fact that the majority of precipitation received in the region is from North American Monsoon System, which is largely unaffected by ENSO (Sheppard et al., 1999). La Niña conditions therefore have the potential to alter the $\delta^{18}\text{O}$ signal in El Malpais precipitation, without necessarily affecting the total annual precipitation amount.

During El Niño conditions, we expect increased Winter precipitation from the Pacific in the Southwest and therefore a decrease in $\delta^{18}\text{O}$ values in precipitation. The opposite effect (a decrease in Winter precipitation) can be found for La Niña events. To confirm this relationship, we have provided a comparison of the $\delta^{18}\text{O}$ records from our ice core and Carlsbad speleothems and the Cave 29 ice core to a reconstruction of the Southern Oscillation Index (SOI_{pr}) based on Pacific precipitation reconstructions using the Mg/Ca ratio in foraminifera (Fig. 8 top black line) (Yan et al., 2011). El Niño like conditions in this scale are inferred by negative SOI_{pr} values, while positive values denote a more La Niña-like state (scale reversed in Fig. 8). Thus, we expect this record to have a direct relationship with $\delta^{18}\text{O}$ in Southwest precipitation, with positive SOI_{pr} values (La Niña-like conditions) resulting in a decrease in Winter Pacific precipitation and therefore an increase in $\delta^{18}\text{O}$. Two major peaks in our record, at AD 540 and 740 align well with strong shifts in SOI_{pr} to La Niña conditions, indicating a decrease in Winter precipitation from the Pacific led to a shift towards positive $\delta^{18}\text{O}$ values. The strong La Niña like conditions around AD ~860 fail to find representation in our record. This could be explained by a lower resolution in our record for this period. It is also possible that a sudden increase in temperature marking the beginning of the MWP resulted in the accelerated increase in $\delta^{18}\text{O}$, masking the effects of this ENSO shift. The Cave 29 ice core $\delta^{18}\text{O}$ values can thus be said to primarily reflect large scale trends in Northern hemisphere temperature, with anomalies in these trends resulting from moisture source variations in response to strong La Niña conditions.

$\delta^{18}\text{O}$ trends in this core reflect a delayed response to variations in the Ljungqvist (2010) multi-proxy reconstruction of Northern hemisphere temperature, decreasing after the transition from the RWP to the DACP, and dramatically increasing after the onset of the MWP.

While the North American Monsoon may have decreased in strength during the DACP, other records such as the pollen study (Follet et al., 2004) in Nevada and the vegetation reconstruction in the Great Plains (Benson et al., 2002) show that different parts of the country experienced increased precipitation from the Pacific during this interval. Since our study area receives a mixture of both Pacific and Gulf of Mexico moisture, a decrease in monsoon strength would not necessarily have led to a decrease in total annual precipitation. In fact, the speleothem record from Carlsbad (Fig. 8 red line) shows relatively wetter conditions during the DACP compared with the onset of the MWP, while average tree-ring growth in the El Malpais record remained stable (Grissino-Mayer, 1995) (Fig. 8 brown line).

Charcoal in the Cave 29 ice core was only present in the upper and lower sections, radiocarbon dated to represent the MWP and the RWP. The presence of abundant charcoal deposits in Cave 29 that coincide with major periods of drought as inferred from our stable isotope analysis, indicate that Native Americans melted the ice for drinking water during such intervals. The lack of charcoal in the middle section that accumulated during the DACP suggests the absence of large-scale ice melting activities by the Ancestral Puebloan during this period. This could be the result of a colder, wetter DACP in the Southwest, as an increase in available drinking water from snowmelt would have eliminated the necessity for cave ice melting practices. It is equally likely that colder temperatures and increased snowfall drove Ancestral Puebloan populations from El Malpais down to lower elevations for this interval. This indicates that while monsoon strength diminished during this interval, annual precipitation in NM increased or remained stable due to an increase in winter precipitation from the Pacific.

References

- Asmerom, Y., Polyak, V.J., Burns, S. & Rasmussen, J. (2007). Solar forcing of Holocene climate: New insights from a speleothem record, southwestern United States. *Geology*, 35, 1-4.
- Benson, L.V. & Berry, M.S. (2009). Climate Change and Cultural Response in the Prehistoric American Southwest. *Kiva* 75: 89-119.
- Blaauw, M. (2010). Methods and code for 'classical' age-modelling of radiocarbon sequences. *Quaternary Geochronology*, 5, 512-518.
- Carrillo, C.M., Castro, C.L., Chang, H.I. & Luong, T.M. (2017). Multi-year climate variability in the Southwestern United States within a context of a dynamically downscaled twentieth century reanalysis. *Climate Dynamics*, 49, 4217-4236.
- Follett, R.F., Kimble, J., Leavitt, S.W. & Pruessner, E. (2004). Potential use of soil C isotope analyses to evaluate paleoclimate. *Soil Science*, 169, 471-488.
- Gat, J.R. (2010). *Isotope Hydrology: A Study of the Water Cycle*. London: Imperial College Press, 6, 189 p.
- Grissino-Mayer, H.D. (1995). *The climate and fire history of El Malpais National Monuments*. Tucson: The University of Arizona, 407 p.

- Ljungqvist, F.C. (2010). A new reconstruction of temperature variability in the extra-tropical Northern Hemisphere during the last two millennia. *Physical Geography*, 92A, 339-351.
- Lowe, J. & Walker, M. (2015). *Reconstructing Quaternary Environments* (2nd ed.). New York: Routledge, 538 p.
- R Development Core Team (2013). (V. A. R Foundation for Statistical Computing, Producer) Retrieved from R: A language and environment for statistical computing: <http://www.r-project.org>
- Rozanski, K., Araguas-Araguas, L. & Gonfiantini, G. (1993). Isotopic Patterns in Modern Global Precipitation. (P. Swart, K. Lohmann, J. Mckenzie & S. Savin, Eds.) *Climate Change in Continental Isotopic Records, Geophysical Monograph Series*, 78, 1-36.
- Sheppard, P.R., Comrie, A.C., Packin, G.D., Angersbach, K. & Hughes, M.K. (1999). *The Climate of the Southwest*. The University of Arizona. Tucson: Institute for the Study of Planet Earth.
- Yan, H., Sun, L., Wang, Y., Huang, W., Qiu, S. & Yang, C. (2011). A record of the Southern Oscillation Index for the past 2,000 years from precipitation proxies. *Nature Geoscience*, 4, 1-4.

Relevant products related to this project:

- Onac, B.P., Parmenter, D., Weaver, E., Baumann, S., Sava, T.B. 2018. Ice deposits in lava tubes of El Malpais National Monument, New Mexico (USA). *Proceedings of the VIII International Workshop on Ice Caves, Potes, Spain*, p. 19.
- Parmenter, D., Onac, B.P., Weaver, E., Baumann, S., Sava, T.B. 2018. *El Malpais Lava Tube ice and guano project: A potential paleoclimate archive for the Southwest*. Best of Karst Event, University of South Florida, Poster Presentation (April 2018)
- Parmenter, D.S. 2018. *Ice and Guano Deposits in El Malpais Lava Tubes: Potential paleoclimate archives for the Southwest United States*. Unpublished Masters Thesis, University of South Florida, 86 p.
- Parmenter, D.S., Baumann, S., Weaver, E., Atudorei, V., Ionita, M., Sava, T.B., Onac, B.P. Hydroclimate variability in the southwestern North America between AD 100 and 1000. To be submitted to *Scientific Reports* journal towards the end of 2019.

We are in the process of producing a short documentary movie (up to 10 minutes) tentatively titled: *Bats, Ice, Lava Tubes, and Climate* (both English and Spanish) with the aim of transferring the scientific results both to a professional and broad general audience. The movie will be played at the Visitor Information centers throughout the park.

A poster deciphering how ice accumulates in lava tubes, what is the source of water, and how ice tells the story of environmental changes will also be prepared and displayed at both visitor centers of ELMA.